
# Statistical Study of Hardware Impairments Effect on mmWave 77 GHz FMCW Automotive Radar

# Statistical Study of Hardware Impairments Effect on mmWave 77 GHz FMCW Automotive Radar

Mohammad Hossein Moghaddam*†, Sina Rezaei Aghdam*, Alessio Filippi† and Thomas Eriksson*
*Department of Electrical Engineering, Chalmers University of Technology, Gothenburg, Sweden
Email: mh.moghaddam@chalmers.se, sinar@chalmers.se, thomase@chalmers.se
† Radar Innovation Group, NXP Semiconductors, Eindhoven, the Netherlands
Email: alessio.filippi@nxp.com

***Abstract*—In this paper, we analyze the effects of hardware impairments on 77GHz FMCW automotive radar performance. Joint in-phase/quadrature imbalance (IQI) and phase noise effects on frequency-modulated continuous-wave (FMCW) radar transceiver front-end are modeled through statistical analysis of distortion and noise. We derive the signal to distortion plus noise ratio, constant false alarm rate, and range-Doppler sensitivity analysis for both the joint and the individual effects of impairments and validate the formulations with simulations. The represented modeling and analysis can be used in millimetre wave (mmWave) FMCW automotive radar signal processing algorithms for optimum transceiver design.**

***Index Terms*—Hardware impairments, phase noise, IQI, additive noise modeling, constant false alarm rate, FMCW automotive radar.**

## I. Introduction

Following the advancement of 5G networks and ever-increasing applications of millimeter wave (mmWave) radio signals, radar sensors data fusion with ultrasound sensors, LiDAR, and cameras are now considered as the main candidates for advanced driver assistant systems (ADASs) as well as autonomous driving (AD). In particular, because of their robustness against adverse lighting and weather conditions, radar sensors are considered a key technology for modern vehicle safety and comfort systems. While autonomous driving using radar sensors is still in the prototype stage, it is expected that by following the trend toward higher automation, more cars will be equipped with radar sensors in the near future comprising the advantages of AD and ADAS systems.

ADASs directly influence the vehicle dynamics, and very strict rules are profiled for maintaining road users' safety in the new regulating functional safety (FuSa) requirements, such as those introduced in the ISO 26262 standard [1]. As an obligation to follow these standards, accuracy and performance of frequency-modulated continuous wave (FMCW) automotive radar systems need to fulfill recommended requirements. One of the most concerning items in FMCW radar design regarding accuracy and performance, is the hardware impairments whose effects are inevitable and need to be analyzed meticulously. Relevant hardware impairments are e.g., non-linear distortions in the power amplifier, phase noise (PN), in-phase and quadrature imbalance (IQI), timing jitter, and spurious emissions. The first step in handling the destructive effects of hardware impairments is to analyze them with the aid of accurate models. Evaluating the performance in terms of impairment parameters and residual effects is studied extensively in both communication [2]–[5] and radar [6]–[12] literature within several different settings. Phase noise, IQI, and oscillator spurs are the most severe hardware impairments in the FMCW radar systems [6], [12]. Signal distortions due to the PN contained in the transmit signal and their effect on the range precision and detection sensitivity are studied in [7]. The impact of PN on the spatial resolution due to variations of signal-to-noise ratio (SNR) and induced limitation on the maximum range estimation is shown in [8]. Authors in [9], explain the range resolution sensitivity in terms of broadened object peak due to deterioration of the PN characteristic. In [10], the authors showed that there may be an additional distortion, caused by the transient response of the phase locked loop, resulting in deviations in sinusoidal nonlinearities in the chirp signal referred to as spurious oscillations (spurs). In [11], the authors represent the effect of IQI in FMCW radar and examine FMCW radars with both IQ mismatch of single channels and mismatch between channels. In [12], authors calculate the Cramer-Rao lower bound (CRLB) of IQI estimation in FMCW radar receivers in terms of gain and phase errors.

In this paper, we will use additive noise modeling introduced in [2], to analyze the joint effect of IQI and phase noise in mmWave FMCW automotive radar. Following the cost-performance trade-off in the mass-production of automotive radar sensors, system designers need to have accurate measures for optimizing the design in the production chain, and for doing so, they need to know the contribution of each hardware impairment effect on the system performance and the resulting cost for compensation in detailed scales. This concern is not fully addressed in the literature, and in this paper, the motivation behind using additive noise modeling is to fulfill the demand for an accurate and tractable measure on the contribution of each hardware impairment on the system performance in both transceiver design and calibration process.

The paper is organized as follows. In Section II, we explain the mmWave FMCW automotive radar system model, and

This work is funded by European union horizon 2020 research and innovation program under the MARIE SKODOWSKA-CURIE agreement No 721732 for Silika project, www.silika-project.eu

978-1-7281-8942-0/20/$31.00 ©2020 IEEE

illustrate the effect of joint IQI and phase noise by using additive noise modeling. In Section III, we validate the analytic study with simulations, and finally, the paper is concluded in Section IV.

## II. Problem formulation

### A. FMCW Automotive Radar System Model

As its name, in frequency-modulated continuous wave radars the transmitted signal is a frequency-modulated signal. Considering linear frequency modulation, the transmitted RF signal can be expressed as

$$s_{\text{RF}}(t) = \exp(j2\pi[f_c + \frac{b}{2}t]t), \tag{1}$$

where $b = B/T$ is the slope of linear modulation considering bandwidth $B$ and pulse duration $T$. In the receiver, the received signal is then multiplied with the conjugated transmit signal (results in the so-called video signal), down-converted and sampled for range-Doppler-angle signal processing. In FMCW radar systems, for estimating the Doppler (velocity estimation), a sequence of $K$ frequency modulated pulses are usually transmitted, and for angle (bearing) estimation, usually a phased array in the transceiver receives the signal. Considering the base-band transmitted signal as

$$s(t) = e^{j\pi bt^2}, \tag{2}$$

the received $k$th chirp in antenna element $n$ reflecting back from $M$ targets after downconversion can be written as [13]:

$$x_{n,k}(t) = \sum_{m=1}^{M} A_m s(t-\tau_m) e^{j2\pi f_{dm} kT} e^{j2\pi f_c \Delta\tau_{m,n}} + \omega_{n,k}(t), \tag{3}$$

where $\tau_m$, $f_{dm}$, and $\Delta\tau_{m,n}$ are the time delay, Doppler shift of the $m$th target, and the delay difference between the antenna array origin and the $n$th antenna for the $m$th target. After multiplication with the conjugated transmit signal and sampling with sampling time $T_s$, the resulting video signal can be obtained as:

$$y[l,k,n] = x_{n,k}(lT_s)s^*(lT_s) =$$

$$\sum_{m=1}^{M} A_m e^{j\pi b\tau_m^2} e^{-j2\pi b\tau_m lT_s} e^{j2\pi T f_{dm} k} e^{j2\pi f_c \Delta\tau_{m,n}} + \tilde{\omega}_{n,k}(lT_s). \tag{4}$$

By considering $\tilde{\omega}_{n,k}(lT_s)$ as zero-mean white Gaussian noise in the base-band, the optimum estimator (reaching the CRLB) of an unknown frequency component in linear frequency modulated exponential observed in finite time interval, is the maximum of the absolute value of its Fourier spectrum [14]. Now to find the desired four frequency component parameters namely range, Doppler, azimuth, and elevation of the target, we need to apply a 4-D FFT on (4), and then finding the maximum in each dimension. The 4-D FFT can be applied as [13]:

$$Y[p,q,\theta,\varphi] = \sum_{n_v=1}^{N}\sum_{n_h=1}^{N}\sum_{k=1}^{K}\sum_{l=1}^{L}$$

$$y[l,k,n] e^{-j2\pi p\frac{l}{L}} e^{-j2\pi q\frac{k}{K}} e^{j2\pi\frac{d}{\lambda}n_h \sin\theta\cos\varphi} e^{j2\pi\frac{d}{\lambda}n_v\sin\varphi}, \tag{5}$$

where $p$, $q$, $\theta$, and $\varphi$ are the arguments of Fourier spectrum for range, Doppler, azimuth, and elevation with $L$ as the total number of samples in one chirp, and $N$ as the total number of antenna elements in each direction of planar array. The planar array is considered as uniform with $n_h$ and $n_v$ as the indices for antenna elements with antenna spacing $d$ in the horizontal and vertical directions in the MIMO radar transceiver, where $n = n_h + H(n_v - 1)$ with $H$ horizontal antennas [13].

By obtaining the four dimensional processed data, the target detection is made through comparing the 4-D data cells with a reference threshold while considering noise level to be known. This method is known as constant false alarm rate (CFAR) in the radar community [14], and automotive radars use CFAR detection considering the following condition:

$$|Y[p,q,\theta,\varphi]|^2 > T + \hat{\sigma}_v^2[p,q,\theta,\varphi], \tag{6}$$

where $T$ is the CFAR threshold and $\hat{\sigma}_v^2[p,q,\theta,\varphi]$ is the noise variance, estimated around the 4-D cell defined by its arguments [13].

### B. Modeling of Phase Noise and IQI in FMCW Radar

The transmitted signal impaired considering phase noise $\varphi(t)$ can be represented by [2]:

$$s_{\text{T}}(t) = e^{j(2\pi f_c t + \varphi(t))} s(t), \tag{7}$$

and then the received signal can be written as:

$$x(t) = Ae^{j(2\pi f_c(t-\tau) + \varphi(t-\tau))} s(t-\tau) + \omega(t), \tag{8}$$

where $\varphi(t)$ is a random walk process. By multiplying (8) with the conjugate of reference signal (7), the video signal can be obtained as:

$$y(t) = s_{\text{T}}^*(t)x(t) =$$

$$Ae^{-j(2\pi f_c t + \varphi(t))} s^*(t)(e^{j(2\pi f_c(t-\tau) + \varphi(t-\tau))} s(t-\tau) + \omega(t))$$

$$= Ae^{j\Delta\varphi(t)}\beta z(t) + \tilde{\omega}(t), \tag{9}$$

where $\Delta\varphi(t) = \varphi(t-\tau) - \varphi(t)$ is a zero-mean wide-sense stationary ergodic process [15], $\tilde{\omega}(t)$ is a zero-mean Gaussian random variable independent from $\Delta\varphi(t)$, $\beta = e^{-j2\pi f_c\tau}$ is a deterministic function of delay, and $z(t)$ is the deterministic base-band video signal defined as:

$$z(t) = s^*(t)s(t-\tau) = e^{j\pi b\tau^2 - j2\pi b\tau t}, \tag{10}$$

and the final base-band signal considering IQI with complex factor $\alpha$ can be represented by:

$$y_{\text{B}}(t) = y(t) + \alpha y^*(t) =$$

$$Ae^{j\Delta\varphi(t)}\beta z(t) + \tilde{\omega}(t) + A\alpha e^{-j\Delta\varphi(t)}\beta^* z^*(t) + \alpha\tilde{\omega}^*(t). \tag{11}$$

By considering $\Delta\varphi(t)$ small enough, we can approximate the exponential of $\Delta\varphi(t)$ with its Taylor expansion and rewrite (11) as [2]

$$y_{\text{B}}(t)\approx$$

$$Az(t) + Aj\Delta\varphi(t)\beta z(t) + \tilde{\omega}(t) - jA^*\alpha\Delta\varphi(t)\beta^* z^*(t)$$

$$-jA^*\alpha\beta^* z^*(t) + \alpha\tilde{\omega}^*(t), \tag{12}$$

Now, we can define the error (distortion) term ($\Pi$) and the desired term ($\Lambda$) as follows

$$\Pi = \tilde{\omega}(t) - jA^*\alpha\Delta\varphi(t)\beta^* z^*(t) - jA^*\alpha\beta^* z^*(t) + \alpha\tilde{\omega}^*(t)$$

$$+jA\Delta\varphi(t)\beta z(t), \tag{13}$$

$$\Lambda = Az(t), \tag{14}$$

Where according to the assumptions on $\Delta\varphi(t)$ and $\tilde{\omega}(t)$ being zero-mean Gaussian random variables, and according to the fact that $z(t)$ is a periodic exponential function and the cross-correlation of a periodic exponential with its conjugate is zero, $\Lambda$ and $\Pi$ become uncorrelated, then we can obtain the power of $\Lambda$ and $\Pi$ as follows

$$\sigma_\Pi^2 = E[\Pi\Pi^*] =$$

$$|A|^2|\alpha|^2|\beta|^2 P_d + E[|\tilde{\omega}(t)|^2 + |\alpha|^2|\tilde{\omega}(t)|^2$$

$$+|A|^2|\beta|^2 P_d\Delta\varphi^2(t)] = \tag{15}$$

$$|A|^2|\alpha|^2|\beta|^2 P_d + (1+|\alpha|^2)\sigma_\omega^2 + |A|^2|\beta|^2 P_d\sigma_\varphi^2,$$

$$\sigma_\Lambda^2 = E[\Lambda\Lambda^*] = |A|^2 P_d, \tag{16}$$

where $P_d = \frac{1}{T}\int |z(t)|^2 dt$ is the power of the deterministic video signal without impairments. Equations (15) and (16) provide a clear picture of how different impairments contribute to the desired signal and the distortion, from where we can analyze the effect of each impairment separately.

To collect all the parameters in a single metric and track them more easily, we can use signal to distortion plus noise ratio (SDNR) [2]

$$\text{SDNR} = \frac{\sigma_\Lambda^2}{\sigma_\Pi^2} \tag{17}$$

We will evaluate the effect of impairments based on analyzing this metric together with CFAR in the simulations.

The CFAR condition based on (6) will not satisfy the presumed probability of detection and false alarm in case of having hardware impairments, consequently. The CFAR condition should be changed according to estimation algorithms and compensation/mitigation scenarios, then, the new CFAR condition will be a function of $\sigma_\Lambda^2$ and $\sigma_\Pi^2$

$$|Y_{\text{HI}}[p,q,\theta,\varphi]|^2 > T(\hat{\sigma}_\Lambda^2, \hat{\sigma}_\Pi^2) + \hat{\sigma}_\Pi^2[p,q,\theta,\varphi], \tag{18}$$

where $Y_{\text{HI}}[p,q,\theta,\varphi]$ is the digital video signal considering hardware impairments, and $\hat{\sigma}_\Lambda^2$ and $\hat{\sigma}_\Pi^2$ are the estimated desired and distortion powers. The threshold $T(\hat{\sigma}_\Lambda^2, \hat{\sigma}_\Pi^2)$ is a function of $\hat{\sigma}_\Lambda^2$ and $\hat{\sigma}_\Pi^2$ which should be determined based on the hardware impairment parameter estimations which by now is out of the scope of this paper and is left to be done in an extension of this paper in future.

## III. Simulation Results and Numerical Analysis

We make the simulation setups to illustrate the effects of IQI and phase noise on the performance of FMCW radar in different scenarios to analyze the effect of each impairment individually and also in combination together. In this way, we define two different scenarios as follows:

- Scenario 1: A single moving target in presence of IQI and phase noise
- Scenario 2: Two moving targets in presence of phase noise without IQI

For both of these scenarios we analyse the range-Doppler map without considering angle estimation, using the following setups:

- Carrier frequency of $f_c = 77$ GHz
- Bandwidth of $B = 300$ MHz
- Pulse duration of $T = 7$ $\mu sec$ (chirp duration)
- 256 FFT beans for range analysis
- 128 FFT beans for Doppler analysis (equal to the number of chirps)
- Hamming window is applied on range FFT beans to reduce sidelobes.
- We have considered probability of false alarm 0.1 % for CFAR detections.

In Fig. 1, the simulation results are presented for Scenario 1, where we have considered both IQI and phase noise for a single moving target. Fig. 1.a, depicts the range-Doppler map for a target in the distance of 80 meter from radar and at the speed of 50 m/s, but due to the effect of IQI, a fake target appears at the distance of 48 m and speed of 210 m/s. Fig. 1.b shows the Doppler and range in separate sweep where we can see the position and speed of the fake target more clearly. In the Doppler sweep, the Doppler spectrum becomes wider and more noisy as we increase the phase noise variance. In Fig. 1.c, the CFAR detection points above the threshold are pointed out for the Range sweep, where the ghost image is detected as a real target.

In Fig. 2, the simulation results are represented for Scenario 2 considering two moving targets. As depicted in Fig. 2.b due to the effect of phase noise, the Doppler spectrum for the two targets are dissolved in each other which makes it

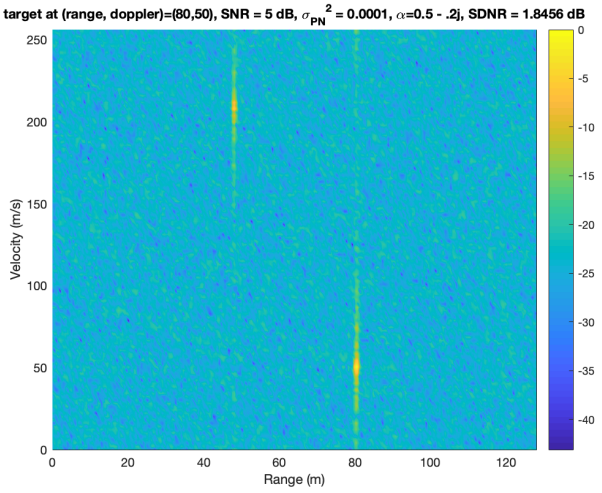


(a)

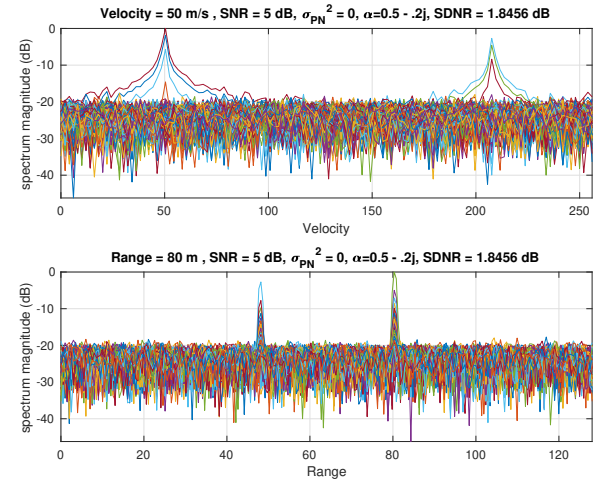


(b)

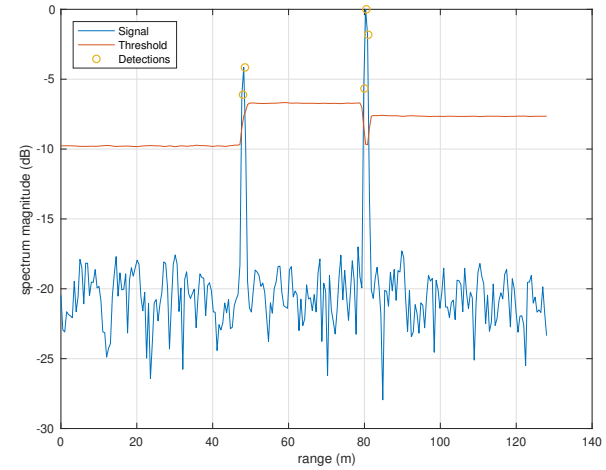


(c)

Fig. 1: Scenario 1, target at (range, velocity)=(80,50), SNR = 5 dB, $\sigma_{\text{PN}}^2 = 0.0001$, $\alpha = 0.5 - 0.2j$, SDNR = 1.8456 dB: a) Range-Doppler map, b) Range and velocity in separate sweeps, c) CFAR detection for probability of false alarm 0.1%.

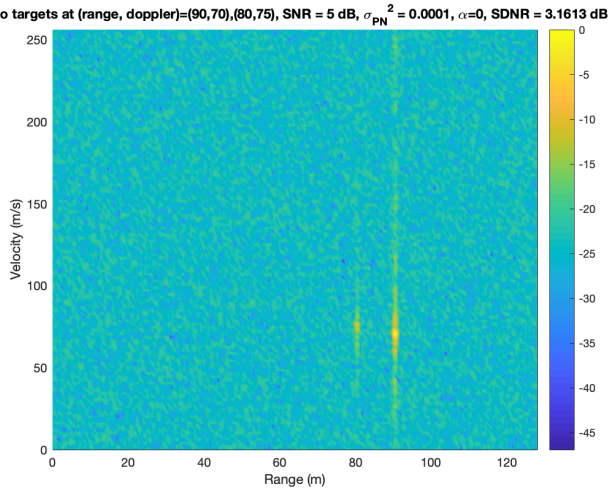


(a)

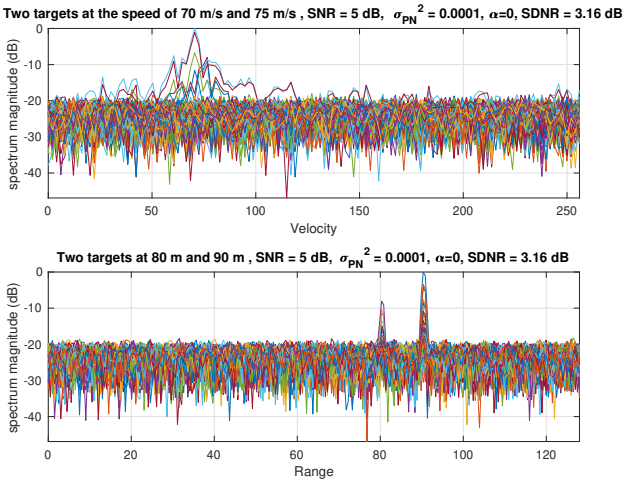


(b)

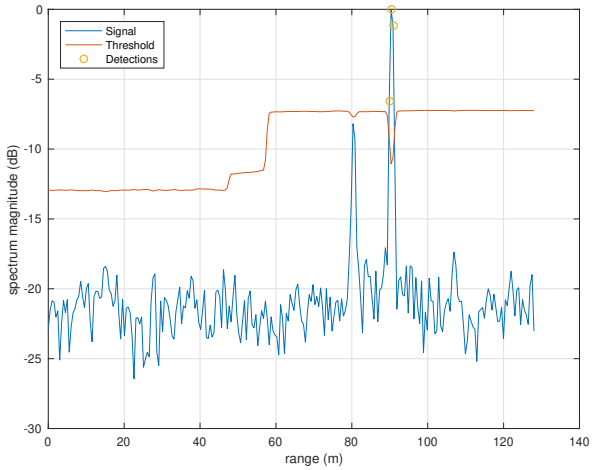


(c)

Fig. 2: Scenario 2, two targets at (range, velocity)=(90,70),(80,75), SNR = 5 dB, $\sigma_{\text{PN}}^2 = 0.0001$, $\alpha = 0$, SDNR = 3.16 dB: a) Range-Doppler map, b) Range and velocity in separate sweeps, c) CFAR detection for probability of false alarm 0.1%.

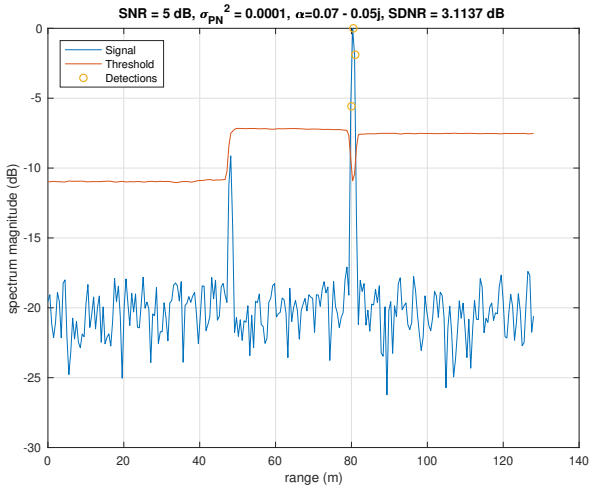


(a)

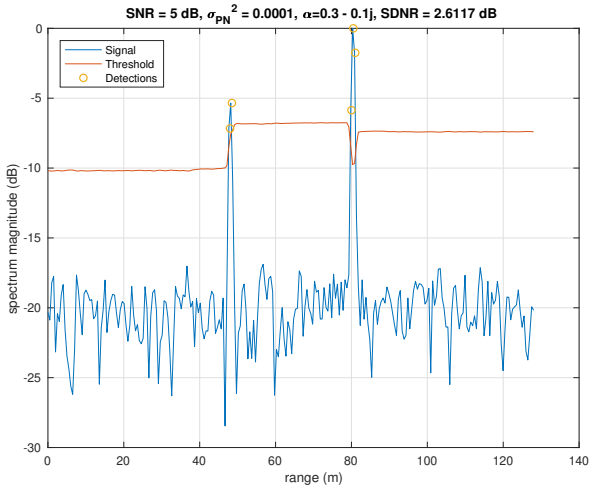


(b)

Fig. 3: Scenario 1, target at (range, Doppler)=(80,50), SNR = 5 dB, $\sigma_{\text{PN}}^2 = 0.0001$ for : a) $\alpha = 0.07 - 0.05j$, SDNR = 3.1137 dB, b) $\alpha = 0.3 - 0.1j$, SDNR = 2.6117 dB.

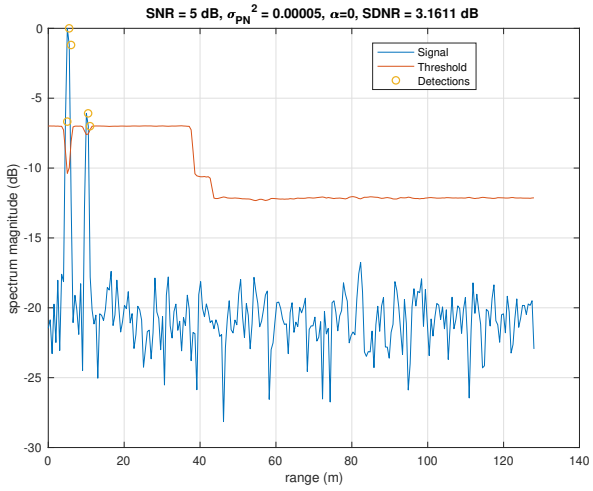


(a)

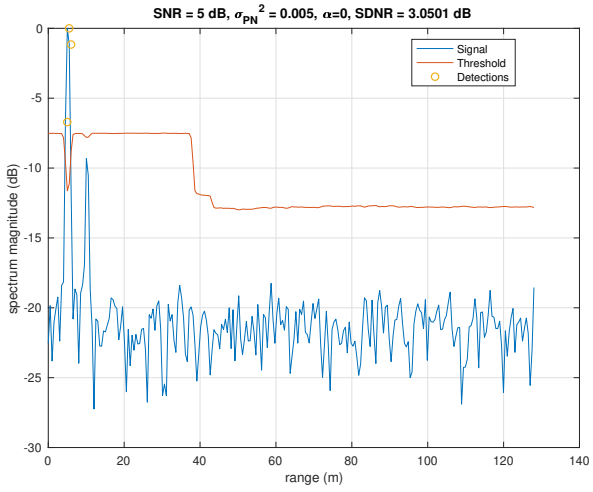


(b)

Fig. 4: Scenario 2, two targets at (range, Doppler)=(5,70),(10,75), SNR = 5 dB, $\sigma_{\text{PN}}^2 = 0.0001$, $\alpha = 0$, for : a) $\sigma_{\text{PN}}^2 = 0.00005$, SDNR= 3.1611, b) $\sigma_{\text{PN}}^2 = 0.005$, SDNR= 3.0501 dB.

difficult to find each target's speed. In Fig. 2.c, the CFAR detection failed to detect the target at 80 m again due to the effect of phase noise. Later in Fig. 4 the effect of phase noise on multi-target detection is explained for different values of phase noise variance. The main message in this paper is that by evaluating (16)-(19), we can have a clear sense about how hardware impairments individually and also in combination can affect the final system performance. In Fig. 3, the CFAR detection for two different IQI factors are depicted addressing two different cases where IQI can affect the detection or not. In case of tracking IQI when we have the knowledge of phase noise variance, it can be traced through (15)-(18) and CFAR algorithms, where to how much extent the IQI factor $\alpha$ can be increased such that the threshold stay above the fake image in the range spectrum. On the other hand, in Fig. 4, CFAR is depicted for two different values of phase noise power, representing the effect of phase noise on the threshold of CFAR detection where it can be seen that in the second case, one of the targets is masked out. In this way, the phase noise variance which can keep the threshold below the desired target level, can be traced by using (15)-(18) and CFAR algorithm similar to the former case for IQI. Details for the parametric tolerance study of CFAR according to hardware impairment components are left to be discussed in an extension of this paper in future.

## IV. Conclusion

In this paper, we have made a statistical study on the effect of hardware impairments on the performance of autonomous

FMCW radar by using additive noise modeling. As the main advantage in comparison with other studies on hardware impairments, the study and modeling presented in this paper can accurately represent the effects of hardware impairments by providing a term-by-term description of their individual and combined effects. As a case study, we have studied the effects of phase noise and IQI for different scenarios of single and multi-target CFAR detection. We have also explained how the current study can be further used for CFAR tolerance study in presence of hardware impairments.

## REFERENCES


[1] "Iso 26262-1:2018 road vehicles — functional safety," 2018.

[2] M. H. Moghaddam, S. R. Aghdam, and T. Eriksson, "An additive noise modeling technique for accurate statistical study of residual rf hardware impairments," in *2019 IEEE International Conference on Communications Workshops (ICC Workshops)*. IEEE, 2019, pp. 1–5.

[3] C. Studer, M. Wenk, and A. Burg, "MIMO transmission with residual transmit-RF impairments," in *Smart Antennas (WSA), 2010 International ITG Workshop on*. IEEE, 2010, pp. 189–196.

[4] S. Jacobsson, U. Gustavsson, G. Durisi, and C. Studer, "Massive MU-MIMO-OFDM uplink with hardware impairments: Modeling and analysis," *arXiv preprint arXiv:1812.02078*, 2018.

[5] A. Georgiadis, "Gain, phase imbalance, and phase noise effects on error vector magnitude," *IEEE Trans. Veh. Technol*, vol. 53, no. 2, pp. 443–449, 2004.

[6] Michael Gerstmair, Alexander Melzer, Alexander Onic, and Mario Huemer, "On the safe road toward autonomous driving: Phase noise monitoring in radar sensors for functional safety compliance," *IEEE Signal Processing Magazine*, vol. 36, no. 5, pp. 60–70, 2019.

[7] Frank Herzel, Dietmar Kissinger, and Herman Jalli Ng, "Analysis of ranging precision in an fmcw radar measurement using a phase-locked loop," *IEEE Transactions on Circuits and Systems I: Regular Papers*, vol. 65, no. 2, pp. 783–792, 2017.

[8] Debashis Dhar, Paul TM van Zeijl, Dusan Milosevic, Hao Gao, and Arthur HM van Roermund, "Modeling and analysis of the effects of pll phase noise on fmcw radar performance," in *2017 IEEE International Symposium on Circuits and Systems (ISCAS)*. IEEE, 2017, pp. 1–4.

[9] M Dudek, I Nasr, D Kissinger, R Weigel, and G Fischer, "The impact of phase noise parameters on target signal detection in fmcw-radar system simulations for automotive applications," in *Proceedings of 2011 IEEE CIE International Conference on Radar*. IEEE, 2011, vol. 1, pp. 494–497.

[10] Serdal Ayhan, Steffen Scherr, Akanksha Bhutani, Benjamin Fischbach, Mario Pauli, and Thomas Zwick, "Impact of frequency ramp nonlinearity, phase noise, and snr on fmcw radar accuracy," *IEEE Transactions on Microwave Theory and Techniques*, vol. 64, no. 10, pp. 3290–3301, 2016.

[11] Michael Ulrich and Bin Yang, "Iq and array calibration for fmcw radar," in *2017 18th International Radar Symposium (IRS)*. IEEE, 2017, pp. 1–10.

[12] Francesco Bandiera, Angelo Coluccia, Vincenzo Dodde, Antonio Masciullo, and Giuseppe Ricci, "Crlb for i/q imbalance estimation in fmcw radar receivers," *IEEE Signal Processing Letters*, vol. 23, no. 12, pp. 1707–1711, 2016.

[13] Igal Bilik, Oren Longman, Shahar Villeval, and Joseph Tabrikian, "The rise of radar for autonomous vehicles: Signal processing solutions and future research directions," *IEEE Signal Processing Magazine*, vol. 36, no. 5, pp. 20–31, 2019.

[14] Mark A Richards, *Fundamentals of radar signal processing*, Tata McGraw-Hill Education, 2005.

[15] Arsenia Chorti and Mike Brookes, "A spectral model for rf oscillators with power-law phase noise," *IEEE Transactions on Circuits and Systems I: Regular Papers*, vol. 53, no. 9, pp. 1989–1999, 2006.